ELSEVIER

Polymer 44 (2003) 451–455

polymer

www.elsevier.com/locate/polymer

Nanostructure of atmospheric and high-pressure crystallized poly(ethylene-2,6-naphthalate). Part II: structure–microhardness correlations

M.C. García Gutiérrez[a,1], D.R. Rueda[a], F.J. Baltá Calleja[a,*], N. Stribeck[b], R.K. Bayer[c]

[a]*Instituto de Estructura de la Materia, CSIC, Serrano 119, 28006 Madrid, Spain*
[b]*Institut f. Technische und Makromolekulare Chemie, Universität Hamburg, Bundesstr. 45, 20146 Hamburg, Germany*
[c]*Institut f. Werkstofftechnik, Universität GH Kassel, Mönchebergstr. 3, 34109 Kassel, Germany*

Abstract

The microhardness of poly(ethylene naphthalene-2,6-dicarboxylate) (PEN), with a detailed characterized nanostructure has been investigated. PEN samples were crystallized from the glassy state at atmospheric pressure and from the melt at high pressure and were characterized using small-angle X-ray scattering (SAXS), wide-angle X-ray scattering (WAXS) and differential scanning calorimetry (DSC). Results show that the degree of crystallinity derived from WAXS, for both atmospheric and high-pressure crystallized PEN, is smaller than that obtained by density and calorimetry. For high-pressure crystallized samples, both, crystallinity and microhardness values are larger than those found for the material crystallized under atmospheric pressure. In the latter case, the hardness values depend on the volume fraction of lamellar stacks within spherulites X_L that depends on the crystallization temperature T_c. For $T_c < 200$ °C, X_L is found to be less than 50%. Thus, for $T_c < 200$ °C a linear relationship between H and T_c is observed provided a sufficiently long crystallization time is used. Results are discussed in terms of the rigid amorphous fraction that appears as a consequence of the molecular mobility restrictions due to the crystal stacks.

Keywords: Poly(ethylene-2,6-naphthalate); Nanostructure; Microhardness

1. Introduction

Poly(ethylene-2,6-naphthalate) (PEN) is a thermoplastic polyester that possesses higher stiffness, better barrier properties and higher melting and glass transition (T_g) temperatures than poly(ethylene terephthalate) (PET). The enhanced mechanical properties of PEN make this polymer attractive for engineering purposes and packaging applications [1,2]. The kinetics of crystallization of PEN, from the glassy state and from the melt, has been studied using real time X-ray scattering methods [3]. We have studied in our laboratory the emerging morphology of PEN during the first stages of crystallization as revealed by electron microscopy [4]. Results on the melting behaviour of PEN [5] and the morphology of high-pressure crystallized PEN have been also recently reported using X-ray scattering methods [6].

The use of microindentation hardness H is now well established as a powerful technique capable to determine changes in morphology and microstructure of polymers that, in turn, are monitoring the macroscopic mechanical properties of these materials [7]. We have shown that the changes in microhardness of PEN also depend on physical aging and on water content [8].

In a preceding paper (first part of the present study) [9], we have investigated the nanostructure of PEN developed after crystallization, both under atmospheric and high-pressure crystallization conditions as revealed by small-angle X-ray scattering (SAXS) and wide-angle X-ray scattering (WAXS). These studies show that during primary crystallization the structure formation process of PEN appears to be governed by thinly scattered volume filling of lamellar stacks. During secondary crystallization the remaining amorphous volume is gradually filled by secondary lamellar stacks. At low crystallization temperatures, there are indications for crystallite insertion into the

* Corresponding author. Address: Instituto de Estructura de la Materia, CSIC, Serrano 119, 28006, Madrid, Spain.
E-mail address: imtb421@iem.cfmac.csic.es (F.J. Baltá Calleja).
[1] Present address: Microfocus Beamline (ID13), European Synchrotron Radiation Facility (ESRF), F-38043 Grenoble, France.

0032-3861/03/$ - see front matter © 2002 Elsevier Science Ltd. All rights reserved.
PII: S0032-3861(02)00777-2

existing stacks. At high crystallization temperatures a rearrangement of the primary stacks during secondary crystallization is observed [9].

The aim of the present study is to examine the nanostructure–microhardness correlation of atmospheric and high-pressure crystallized PEN as a function of temperature and crystallization time, as well as of crystallization pressure.

2. Experimental

Experimental details concerning materials and samples preparation are given in Ref. [9]. Two set of samples were investigated:

(a) *PEN samples crystallized at atmospheric pressure*. Glassy PEN films (0.3 mm thick) were crystallized beyond the primary crystallization at different temperatures ($T_c = 165$, 180, 220 and 245 °C). Crystallization times t_c range from 0.5 to 300 h.

(b) *High-pressure crystallized PEN samples*. PEN pellets were melted in a cylindrical mould at different temperatures (300, 320, 330 and 340 °C) and then crystallized under a pressure of 400 MPa for 1 h. These samples appear in the form of 2 mm thick disks having a diameter of 20 mm.

The structural characterization of samples was achieved by means of X-ray diffraction (WAXS and SAXS), differential scanning calorimetry (DSC) and density (ρ) measurements, as described previously [9]. Structural parameters of both sets of samples derived from WAXS, DSC and density, are collected in Tables 1 and 2. The parameters determined from SAXS, from the analysis of the interface distribution function (see part 1, Ref. 9) allow a detailed nanostructure characterization of the material, namely the crystal thickness l_c, amorphous layer thickness, l_a and the width of the transition zone, t_i. The linear

Table 1
Nanostructure parameters for atmospheric pressure-crystallized PEN

T_c (°C)	t_c (h)	X_{cW}	$X_{c\rho}$	l_c (nm)	l_a (nm)	t_i (nm)	X_{cL}	X_L
165	2	0.22	0.24	4.6	3.0	1.4	0.61	0.41
	24	0.22	0.25	4.4	3.0	1.4	0.59	0.44
180	0.5	0.21	0.25	5.3	3.0	1.4	0.64	0.41
	2	0.21	0.27	4.5	3.3	0.9	0.58	0.48
	24	0.22	0.27	4.9	2.8	1.2	0.63	0.48
220	0.5	0.24	0.33	6.6	4.2	1.4	0.61	0.56
	2	0.30	0.37	7.6	4.0	1.5	0.66	0.58
	24	0.28	0.38	6.9	4.3	1.1	0.61	0.64
245	0.5	0.26	0.38	8.5	5.9	1.2	0.59	0.66
	2	0.27	0.41	8.0	5.5	1.1	0.59	0.71
	24	0.32	0.44	7.1	5.6	1.0	0.56	0.80

Table 2
Nanostructure parameters for high-pressure crystallized PEN

T_c (°C)	X_{cW}	$X_{c\rho}$	X_{cDSC}	l_c (nm)	l_a (nm)	t_i (nm)	X_{cL}	X_L
300	0.42	0.57	0.54	6.7	4.4	1.1	0.60	0.95
320	0.43	0.61	0.60	7.2	3.6	1.0	0.67	0.91
330	0.53	0.65	0.63	7.2	3.1	0.8	0.70	0.93
340	0.43	0.56	0.54	7.5	3.9	1.2	0.66	0.85

crystallinity within lamellar stacks X_{cL}, is defined as [10]:

$$X_{cL} = \frac{l_c}{l_c + l_a} = \frac{l_c}{L} \quad (1)$$

and the volume fraction of stacks within the spherulites X_L, as:

$$X_L = \frac{X_c}{X_{cL}} \quad (2)$$

where X_c is the volume crystallinity. Here we have used as X_c the crystallinity derived from density, $X_{c\rho}$.

Microhardness H, was determined at room temperature using a Leitz microhardness tester together with a Vickers square-based pyramidal diamond indenter. The H value (in MPa) was derived from the residual area of impression using the equation $H = Kp/d^2$, where d is the mean diagonal length of the indentation in m, p is the applied force in N and K is a geometrical factor equal to 1.854 [7]. Loads of 0.10, 0.15 and 0.25 N to correct for the instant elastic recovery were used. About 10 indentations were averaged for each hardness value. The force was applied at a controlled rate, held for 0.1 min and, then, removed. The length of the impression is measured to ±0.5 μm.

3. Results and discussion

3.1. Crystallization at atmospheric pressure

3.1.1. Variation of microhardness with temperature and crystallization time

From the data of Table 1, one observes that crystallinity increases with temperature and time of crystallization from approximately 0.2 to 0.4. It is to be noted that the values of the degree of crystallinity from WAXS are smaller than those obtained by density. In case of PET this disparity is outside of experimental error [11], and apparently increases with increasing the degree of crystallinity. The lower values of the degree of crystallinity from WAXS as compared with those derived from the density measurements has been explained by assuming the occurrence of an interface of finite thickness between the crystals and the amorphous regions [11]. This interphase or transition zone, would not be seen as crystalline by the X-ray scattering experiment, however this region may have a higher density as compared to the amorphous domains.

Fig. 1 shows the variation of H with crystallization

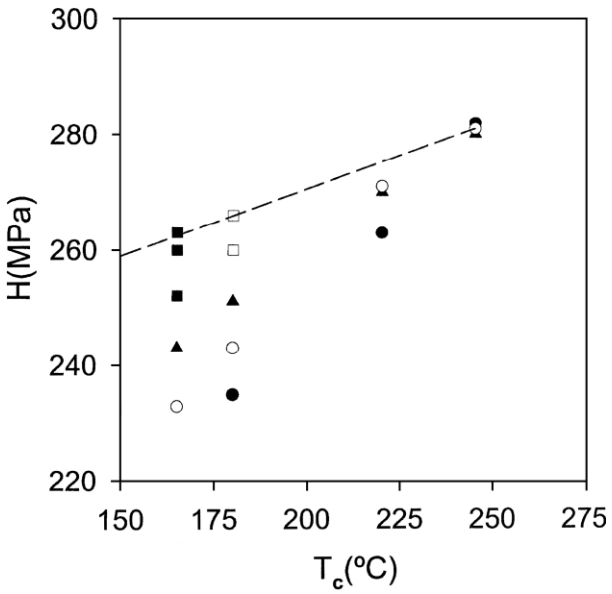

Fig. 1. Variation of microhardness H, during secondary crystallization, with crystallization temperature, for different times: (●) $t_c = 0.5$ h, (○) $t_c = 2$–3 h, (▲) $t_c = 24$ h; (■, □) long t_c values (up to more than 300 h).

temperature for different times. Results show that for each temperature H increases with increasing crystallization time, t_c. However, the range of hardness variation becomes gradually smaller with increasing T_c. For $T_c = 245$ °C, the highest crystallization temperature reached ($X_L > 66\%$), the H-value is nearly independent of t_c. In addition, H seems to reach an upper limit that linearly increases with increasing T_c (dashed line in Fig. 1).

Generally, the hardness of a polymer can be described in terms of a parallel model of alternating amorphous and crystalline regions, following [7]:

$$H = H_c X_c + H_a(1 - X_c) \tag{3}$$

where H_c and H_a are the hardness values of crystalline and amorphous regions, respectively, and X_c is the volume fraction of crystallinity. Since for the secondary crystallization regime, $X_c = X_L X_{cL}$ [10], then Eq. (3) can be written:

$$H = H_c(X_L X_{cL}) + H_a(1 - X_L X_{cL}). \tag{4}$$

When the volume fraction occupied by lamellar stacks inside the spherulite volume, $X_L < 50\%$ the amorphous regions are sufficiently large and the hardness value of the amorphous material corresponds to H_a. However, when X_L exceeds 50%, the amorphous regions become occluded within the lamellar stacks and it is known that the molecular mobility in stiff polymers decreases behaving as a rigid amorphous phase [12]. Owing to these restrictions in molecular mobility one might assume that the hardness of the rigid amorphous regions becomes closer to that of the crystals, i.e. much larger than that of the amorphous material without restrictions. Thus, for cystallization temperatures T_c above 200 °C, particularly for $T_c = 245$ °C, according to Eq. (3) when $H_a \sim H_c$, then H remains constant and independent of t_c although the volume crystallinity continues increasing with increasing crystallization time.

3.1.2. Structure–microhardness correlation

Eq. (4) indicates that the volume fraction of crystalline material controls the microhardness of the polymer. However, the dependence of H_c upon the crystal thickness l_c is also known [7]. Based on a thermodynamic approach an expression that predicts such a dependence, assuming a heterogeneous plastic deformation of the crystals under the indenter, has been derived [13]:

$$H_c = \frac{H_c^{\infty}}{1 + (b/l_c)} \tag{5}$$

where H_c^{∞} is the hardness for an infinitely thick crystal and $b = 2\sigma_e/\Delta h$ is a parameter related to the surface free energy σ_e of the crystals and to the energy Δh required for plastic deformation of the latter. After rearranging Eq. (5) one obtains:

$$\frac{1}{H_c} = \frac{1}{H_c^{\infty}} + \frac{b}{H_c^{\infty}}\frac{1}{l_c}. \tag{6}$$

Fig. 2 illustrates the variation of $1/H_c$ with $1/l_c$ (in the derivation of the H_c values an experimental value of $H_a = 182$ MPa was used). The data in Fig. 2 segregate into two groups depending on l_c. According to Eq. (6) each group of data fit into a straight line of slope b/H_c^{∞} yielding a common intercept corresponding to a value of $H_c^{\infty} = 860$ MPa, in accordance with data found for copolyesters of PEN [14]. For samples with a crystal thickness $l_c > 6$ nm ($T_c > 200$ °C), from the slope we can estimate a value of $b = 7.7$ nm which corresponds to the value found for the

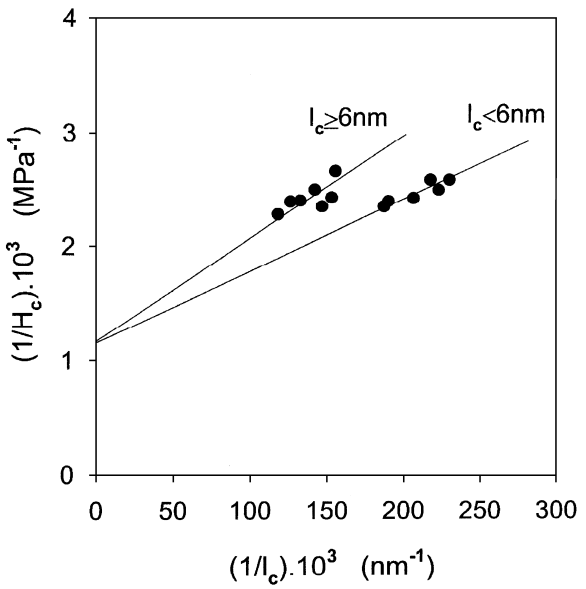

Fig. 2. Plot of H_c^{-1} as a function of l_c^{-1} for atmospheric pressure crystallized PEN.

α-phase PEN crystals [14]. On the other hand, for samples with a crystal thickness $l_c < 6$ nm ($T_c < 200$ °C) we obtain a value of $b = 5.5$ nm. The obtained increase of the b-value with increasing crystallization temperature suggests that the surface free energy (which is proportional to the density of surface defects [13]) increases with T_c. The b-increase might be related to the formation of a rigid interface layer between the crystallites and the amorphous regions. A similar effect was found in poly(ethylene terephthalate) [15].

3.2. Crystallization at high pressure

3.2.1. Variation of microhardness with crystallization temperature

Table 3 shows that H increases with increasing T_c under high pressure, except for the highest temperature where partial melting may occur, yielding a lower crystallinity value [9]. Nevertheless all the PEN samples crystallized under high pressure show higher crystallinity values than the atmospheric pressure crystallized ones (compare Tables 1 and 2). Although the crystallinity values are high (Table 2), they are however, considerably lower than those corresponding to PET samples crystallized under similar conditions [11,16]. Again, the values of the degree of crystallinity obtained from WAXS are smaller than those obtained by density and by DSC. The difference is even larger than for atmospheric pressure crystallized PEN. As pointed out above, the lower X_{cW}-values can be explained assuming that there exists an interface of finite thickness between the crystals and the amorphous regions. The thickness of the interface obtained from the SAXS data analysis is $t_i \approx 1.0$ nm, i.e. close to the value calculated for atmospheric pressure crystallized PEN. However, from the structural parameters of the two-phase system presented in Table 2 it is seen that the fraction occupied by lamellar stacks inside the spherulites ($X_L \approx 0.90$) and, hence, the amount of material that belongs to the interface is larger for high-pressure crystallized PEN. This finding justifies the larger disparity between the values of the degree of crystallinity obtained by WAXS and by the other techniques.

3.2.2. Nanostructure–microhardness correlation

By combination of Eqs. (3) and (5) we can rewrite the hardness as:

$$H = \lfloor (H_c^{\infty}/1 + (b/l_c)) - H_a \rfloor X_c + H_a. \quad (7)$$

Table 3
Microhardness and crystal hardness of PEN crystallized under high pressure for 1 h at different temperatures

T_c (°C)	300	320	330	340
H (MPa)	320	341	352	325
H_c (MPa)	424	443	444	437

In order to examine the double dependency of H upon X_c and l_c we have shown in Fig. 3 the variation of H vs. X_c and taking l_c as parameter according to Eq. (7). The straight lines for different l_c values are drawn using the H_c^{∞} and b values derived above in Fig. 2, i.e. $H_c^{\infty} = 860$ MPa and $b = 5.5$ nm (for $l_c < 6$ nm) and $b = 7.7$ nm (for $l_c > 6$ nm). The experimental data for both, atmospheric (filled symbols) and high-pressure (open symbols) crystallized PEN samples are also shown in Fig. 3. It is worth noticing the linear relationship between H and $X_{c\rho}$ for both types of crystallized PEN samples.

4. Conclusions

1. For PEN crystallized under atmospheric pressure the microhardness is linearly related to the isothermal crystallization temperature provided the secondary crystallization is almost completed. Thus for the lowest T_c (165 °C) investigated, the crystallization times t_c required to obtain limiting H values are considerably long (up to 300 h) in contrast to the short t_c values (~0.5 h) necessary at the highest T_c (245 °C).
2. In the range of T_c investigated two different morphologies are developed, depending on whether X_L is smaller or larger than 50%, giving rise to different crystal hardness values. The hardness of infinitely thick PEN crystals has been calculated to be 860 MPa.
3. Crystallization of PEN under high-pressure yields harder and more crystalline materials than those crystallized at atmospheric pressure. In addition, for both types of samples we find that the microhardness is linearly related to the degree of crystallinity, which increases with the amount of crystalline stacks within the spherulites.

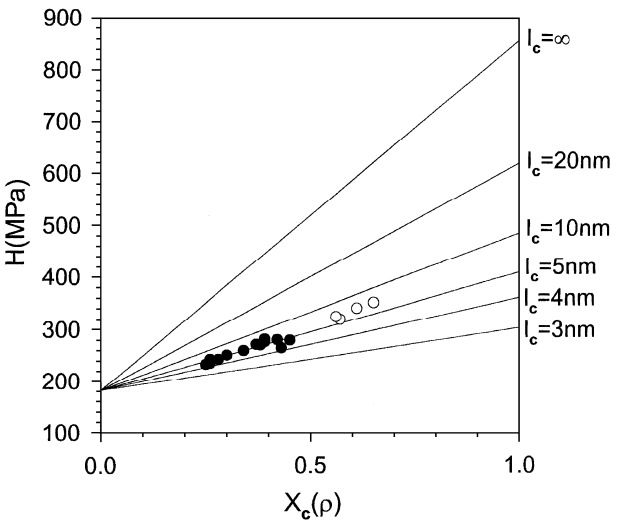

Fig. 3. H variation with X_c for atmospheric (solid symbols) and high-pressure (open symbols) crystallized PEN. The straight lines follow Eq. (7) (see text).

Acknowledgements

Grateful acknowledgement is due to MCYT, Spain (Grant BFM2000-1474), for the generous support of this investigation.

References

[1] Ghahem AM, Porter RS. J Polym Sci Polym Phys Ed 1989;17:480.
[2] García Gutiérrez MC, Karger-Kocsis J, Riekel C. Macromolecules 2002;35:7320.
[3] Buchner S, Wiswe D, Zachmann HG. Polymer 1989;30:480.
[4] Baltá Calleja FJ, Rueda DR, Michler GH, Naumann I. J Macromol Sci Phys 1998;B37:411.
[5] Denchev Z, Nogales A, Sics I, Ezquerra T, Baltá Calleja FJ. J Polym Sci, Polym Phys Ed 2001;39:881.
[6] Li L, Wang C, Huang R, Zhang L, Hong S. Polymer 2001;42:8867.
[7] Baltá Calleja FJ, Fakirov S. Microhardness of polymers. Cambridge: Cambridge University Press; 2000.
[8] Rueda DR, Varkalis A, Viksne A, Baltá Calleja FJ, Zachmann HG. J Polym Sci Polym Phys Ed 1995;33:1653.
[9] García Gutiérrez MC, Rueda DR, Baltá Calleja FJ, Stribeck N, Bayer RK. J Mater Sci 2001;36:5739.
[10] Zachmann HG, Wutz C. In: Dosiére M, editor. Crystallization of polymers. Dordrecht: Kluwer; 1993. p. 403.
[11] Köncke U, Zachmann HG, Baltá Calleja FJ. Macromolecules 1996; 29:6019.
[12] Huo P, Cebe P. Macromolecules 1992;25:902.
[13] Baltá Calleja FJ, Santa Cruz C, Bayer R, Kilian HG. Coll Polym Sci 1990;268–440.
[14] Baltá Calleja FJ, Santa Cruz C, Chen D, Zachmann HG. Polymer 1991;32:2252.
[15] Santa Cruz C, Baltá Calleja FJ, Zachmann HG, Stribeck N, Asano T. J Polym Sci, Polym Phys 1991;29:819.
[16] Stribeck N, Zachmann HG, Bayer RK, Baltá Calleja FJ. J Mater Sci 1997;32:1639.